Canadian Conference - Pacific Conference on Earthquake Engineering 2023
Vancouver, British Columbia
June 25th – June 30th, 2023

Effects of model fitting techniques on predicted lateral response of UFREIs: one-cycle vs. all-cycle fitting

Hediyeh Sheikh[1], Noor Hasan[2], Rajeev Ruparathna[3], and Niel C. Van Engelen[3*]

[1]PhD Student, Department of Civil and Environmental Engineering, University of Windsor, Ontario, Canada
[2]Undergraduate Student, Department of Civil and Environmental Engineering, University of Windsor, Ontario, Canada
[3]Assistant Professor, Department of Civil and Environmental Engineering, University of Windsor, Ontario, Canada
*Niel.VanEngelen@uwindsor.ca (Corresponding Author)

ABSTRACT

Elastomers are well-suited for utilization as base isolators owing to their ability to accommodate large recoverable strains. Incorporation of reinforcement, such as steel or fibers, into an elastomer composite takes advantage of the near incompressibility of the elastomer, which enhances the vertical and bending properties of the bearing. Despite the similarity in the conceptual design of fiber-reinforced and steel-reinforced elastomeric bearings, the lateral direction exhibits distinct performance characteristics due to the fiber reinforcement's lack of flexural rigidity. Fiber-reinforced elastomeric isolators (FREIs) can be placed bonded or unbonded between the upper and lower supports of a base isolated structure. The unbonded application of FREIs is favourable due to the unique rollover deformation that occurs with lateral displacement. This particular behaviour leads to a distinct change in the lateral response of unbonded FREIs (UFREIs). Finding an appropriate numerical model that accurately captures this adaptive behaviour is challenging. There are several numerical models that can be used for representing the behaviour of UFREIs. In each case, the model parameters need to be calibrated using the results of experimental programs. The parameters can be fitted to all cycles of experimental data, or depending on the research interest, to one cycle (i.e., expected displacement demand in the earthquake). In this study, the effect of fitting techniques (one-cycle vs. all-cycle) on the response of the UFREIs was evaluated. Previous lateral cyclic and shake table tests were employed to compare each approach. The effective lateral stiffness, equivalent viscous damping, and area of cyclic loading test and the peak displacement responses of shake table test are used to compare the results of each set of parameters for each model. The results indicate that one-cycles fitting yields better outcomes in low expected displacement demand, while the all-cycle fitting method proves to be more suitable for high displacement demand.

Keywords: Unbonded fiber-reinforced, algebraic model, numerical modeling, fitting technique, Shake table verification.

INTRODUCTION

Seismic base isolation is an increasingly prevalent approach for mitigating earthquake-induced losses. Its primary objective is to decouple structures, such as buildings and bridges, from strong ground motions by introducing a flexible layer at the foundation [1]. This technique has been established as an effective means of protecting both the structure and its contents from damage resulting from earthquakes. Elastomers are favoured materials for base isolation due to their soft properties and ability to endure large recoverable strains [2], [3]. Although steel-reinforced elastomeric isolators (SREIs) have been widely employed, their weight and cost have been perceived as impediments to the widespread application of base isolation. To alleviate these concerns, it has been suggested to substitute steel reinforcement with lighter fiber reinforcement possessing comparable tensile properties [4]. Fiber-reinforced elastomeric isolators (FREIs) are viable and possess desirable characteristics. As an additional cost-saving measure, researchers have recommended placing the FREI in an unbonded state between the upper and lower supports [2]. This approach results in a rollover deformation under horizontal displacement, resulting in a nonlinear force-displacement relationship characterized by both a softening and a stiffening phase. This nonlinear relationship is advantageous, as it allows the device's performance to be tailored to the level of earthquake hazard [5], [6]. FREIs can be cut to the desired size from larger pads and are designed by considering the extensibility and lack of flexural resistance of the fiber reinforcement, in addition to the compressibility of the elastomer [4].

The force-displacement relationship of an unbonded FREI (UFREI) is characterized by softening and stiffening regimes due to the rollover effect. This phenomenon (i.e., rollover) occurs when the end sections of the isolator lose contact with the upper and lower supports as lateral displacements are applied, shown in Figure 1a. The rollover sections rotate until the initially vertical faces of the bearing rotate 90º and contact the supports, known as full rollover (Figure 1b). The load-displacement relationship under lateral loading can be divided into three distinct regions: an initial near-linear region, a softening region, and a subsequent stiffening region. During the initial region, the isolator displays near-linear elastic behaviour. The softening region is characterized by a reduction in effective lateral stiffness due to rollover, resulting in a more efficient device by moving the fundamental period further away from the critical high-energy range of typical earthquake events. In the stiffening region, there is an increase in effective stiffness, which acts as a self-restraint mechanism to prevent excessive displacements during extreme events [5], [7].

There have been different techniques employed to develop numerical models for the purpose of non-linear time history analysis of UFREIs. These models exhibit distinguishing features with respect to their accuracy, computational efficiency, and the number and mechanical significance of the parameters utilized. The numerical models used to simulate UFREIs can be categorized into two major types based on the equation used to determine the output variable (usually lateral force) [8]. The first type is differential models, which employ differential equations to describe the rate of change of force and displacement. The second type is algebraic models, which directly relate the force and displacement variables using mathematical equations.

In terms of differential models, the Bouc-Wen (BW) model is a commonly used method for simulating the hysteretic load-displacement behaviour of various structural elements [9]. The original model was first introduced by Bouc [10] and subsequently improved by Wen [11] to include a range of hysteretic features. Unlike other models, the BW model utilizes a single non-linear differential equation to describe a smooth hysteretic behaviour without differentiating between various phases of the loading pattern [12]. Furthermore, an algebraic model introduced by Vaiana et al. [8] can also be used to simulate the hysteretic behaviour of rate-independent mechanical systems and materials. The model accurately predicts the behaviour of UFREIs while requiring less computational effort due to the absence of an ordinary differential equation (ODE) to solve and fewer parameters to fit compared to differential models like BW models.

In this study, the effect of fitting techniques (one-cycle vs. all-cycle) on the response of UFREIs is evaluated. Due to the highly non-linear nature of UFREIs, an iterative approach could be used in time history analysis where the model parameters are selected based on the cycle with a displacement amplitude closest to the maximum displacement. This approach, however, is time consuming and computationally expensive as it requires the model to be run several times. Alternatively, the model parameters could be fitted based on all displacement cycles simultaneously. However, in this case, the model fit over individual cycles may be poorer and contribute to increased error. The algebraic model [8] was chosen as the considered numerical model and fitted to experimental data using particle swarm optimization to identify its parameters. The parameters were obtained by fitting the model to either all cycles (i.e., all tested displacement amplitudes) of experimental data or a specific cycle (i.e., specific displacement amplitude). To assess the effectiveness of each approach, the results of previous lateral cyclic and shake table tests that were conducted on a quarter-scale UFREI base-isolated structure [13] were considered. The effective lateral stiffness, equivalent viscous damping, and area of each cycle area enclosed within each cycle of cyclic loading test and the peak responses of shake table test were used to compare each approach.

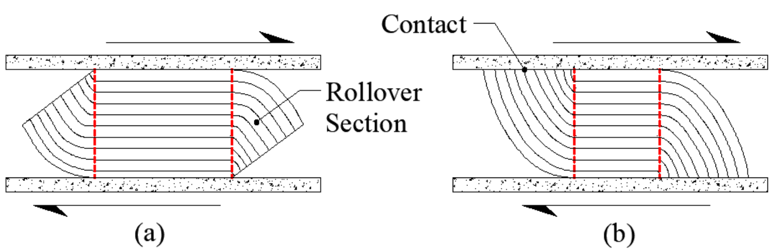

Figure 1. Lateral displacement of an UFREI illustrating (a) rollover and (b) full rollover.

BACKGROUND: ALGEBRAIC MODEL

Vaiana et al. [8] developed an algebraic model for predicting the hysteretic behaviour of UFREIs. This model is based on an algebraic equation to calculate the isolator restoring force. Hence, it is referred to as the algebraic model (AM). The AM characterizes a typical force-displacement hysteresis loop using four types of curves, which comprise of two parallel limiting curves (c_u and c_l), and the loading and unloading curves (c^+ and c^-), shown in Figure 2. This model employs five parameters, namely k_a, k_b, α, β_1, and β_2. The size and/or shape of the hysteresis loop is impacted by each parameter of the model. The authors provided a detailed explanation of the formulation of the AM and the effect of its parameters on the size and/or shape of the hysteresis loops. To simplify the computer implementation of the AM, Vaiana et al. [8] presented a summary of the process in their publication as follows:

1. Initial settings
   1.1. Set the five model parameters: k_a, k_b, α, β_1, and β_2
   1.2. Compute the internal model parameters

$$u_0 = \frac{1}{2}\left[\left(\frac{k_a - k_b}{\delta_k}\right)^{\frac{1}{\alpha}} - 1\right] \tag{1}$$

$$\bar{f} = \frac{k_a - k_b}{2}\left[\frac{(1 + 2u_0)^{(1-\alpha)} - 1}{1 - \alpha}\right] \tag{2}$$

where δ_k can be set to 10^{-20} based on the Vaiana et al. [8] suggestion.

2. Calculations at each time step
   2.1. If $s_t s_{t-\Delta t} < 0$, update the history variable

$$u_j = u_{t-\Delta t} + s_t(1 + 2u_0) - s_t\left\{\frac{s_t(1-\alpha)}{k_a - k_b}\left[f_{t-\Delta t} - \beta_1 u_{t-\Delta t}^3 - \beta_2 u_{t-\Delta t}^5 - k_b u_{t-\Delta t} - s_t\bar{f} + (k_a - k_b)\frac{(1+2u_0)^{(1-\alpha)}}{s_t(1-\alpha)}\right]\right\}^{\left(\frac{1}{1-\alpha}\right)} \tag{3}$$

   2.2. Evaluate the restoring force at time t

if $u_j s_t - 2u_0 \leq u_t s_t < u_j s_t$:

$$f_t = \beta_1 u_t^3 + \beta_2 u_t^5 + k_b u_t + (k_a - k_b)\left[\frac{\left(1 + s_t u_t - s_t u_j + 2u_0\right)^{(1-\alpha)}}{s_t(1-\alpha)} - \frac{(1+2u_0)^{(1-\alpha)}}{s_t(1-\alpha)}\right] + s_t\bar{f} \tag{4}$$

else:

$$f_t = \beta_1 u_t^3 + \beta_2 u_t^5 + k_b u_t + s_t\bar{f} \tag{5}$$

where s_t is the sign of the velocity at time t (i.e., sgn($\dot{u}_t$)), u_t and f_t are displacement and restoring force at time t, respectively, and u_j is a history variable which is shown in Figure 2. This variable must be updated if there is a change in the velocity sign during the time interval.

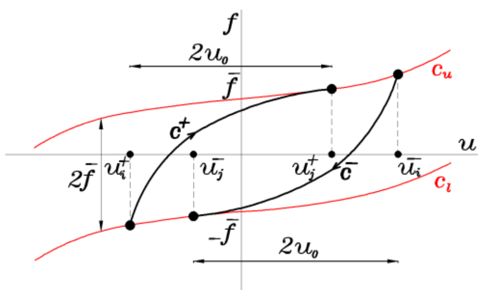

Figure 2. Sketch of the four AM curves: c_u, c_l, c^+, and c^- [8].

METHODOLOGY

Experimental data

The data for the study were collected from prior lateral cyclic testing and shake table testing conducted on a quarter-scale UFREI base isolated structure conducted by Foster [13]. The UFREI specimen had a square cross-section of 63 mm x 63 mm and comprised a total thickness of elastomeric layers, t_r, of 19.05 mm. The experiment involved subjecting the UFREI specimen to three fully reversed sinusoidal cycles at seven different horizontal displacement amplitudes ascendingly ranging from 0.25 t_r to 2.50 t_r. The average rate was 76.2 mm/s, which corresponds to a frequency of 1 Hz at 1.00 t_r. The elastomer material was identified as neoprene rubber, with a nominal tensile modulus of 1.0MPa at 100% elongation and a specified shear modulus of G=0.35MPa, as per the manufacturer's specifications [13].

The shake table testing program utilized the El Centro (1940) ground motion record as one of the input motions, which is considered herein [13]. To cover a broad spectrum of earthquakes occurring in eastern and western Canada, Foster [13] scaled the peak ground acceleration (PGA) of each considered earthquake record from 0.1g to 0.5g with an increment of 0.1g. Since the shake table testing had been performed on unscragged specimens with the same characteristics as used in the cyclic loading test, the fitted parameters from the cyclic test were employed.

Fitting techniques

In this study, a methodology was developed to evaluate the effect of fitting techniques (one-cycle vs. all-cycle) on the response of UFREIs under seismic loading. To identify the parameters of the numerical model used in this study, i.e., AM, Particle Swarm Optimization (PSO) was employed. The PSO algorithm is a computational optimization technique that is inspired by the social behavior of bird flocking or swarms of insects. It is a population-based algorithm that optimizes a problem by iteratively enhancing a candidate solution in terms of a predicted quality. PSO involves a set of candidate solutions, referred to as particles, that traverse the search space and adjust their position based on their individual experiences and those of their neighbours. The quality of a particle's current position is evaluated using an objective function, and particles communicate their best-known positions with each other. The algorithm progresses by iteratively updating the velocity and position of each particle with the objective of converging towards the global optimal solution [14]–[16]. The objective function for identifying the parameters of the AM employs the method of minimizing the force residuals. This technique involves minimizing the difference between the observed response, derived from experiments, and the anticipated response, obtained from a computed curve.

The parameters of the AM were fitted to the experimental hysteresis loops obtained through cyclic lateral testing using two methods: fitting to all cycles and fitting to one cycle. In all-cycle fitting, the numerical model parameters were estimated considering all cycle displacement amplitudes simultaneously. While in one-cycle fitting, the model parameters were obtained by fitting the model to the cycle closest to the displacement demand in the earthquake (i.e., the maximum displacement amplitude reached in the shake table test for the specific earthquake record). The AM parameters obtained by fitting to all cycles and one amplitude cycle, which represents the expected displacement demand for each PGA value, were used in the time history analysis. For the one-cycle fitting, the fitting parameters to 0.50 t_r, 0.75 t_r, 1.00 t_r, 1.50 t_r, and 2.00 t_r were used for the time history analysis under the earthquake with PGAs 0.1g, 0.2g, 0.3g, 0.4g, and 0.5g, respectively.

Evaluation techniques

The effective lateral stiffness (Eq. (6)), equivalent viscous damping (Eq. (7)), and area of each cycle area enclosed within each cycle of cyclic loading test and the peak responses of shake table test were used to evaluate each approach.The effective lateral stiffness, k_L, was determined as [17]:

$$k_L = \frac{F_{L,\max} - F_{L,\min}}{u_{\max} - u_{\min}} \tag{6}$$

where $F_{L,max}$ and $F_{L,min}$ are the maximum and minimum lateral force observed over the cycle, and u_{max} and u_{min} are the maximum and minimum displacement observed over the same cycle, respectively.

The equivalent viscous damping, ζ_L, has been determined as [17]:

$$\zeta_L = \frac{2W}{\pi k_L \left(u_{\max} - u_{\min}\right)^2} \tag{7}$$

where W is the area enclosed within the hysteresis loop of the considered cycle.

The time-history analysis was conducted using OpenSees [18] in two dimensions. The beams and columns were modeled using elastic beam-column elements and were assumed to be axially rigid. The largest positive and negative displacement peaks and the normalized experimental and model hysteretic loops at different PGA values were used to compare the estimation error of the models to experimental data.

RESULTS

Cyclic lateral testing

The model-to-experimental ratios for all-cycle and one-cycle fitting for the effective lateral stiffness, equivalent viscous damping, and the area enclosed within the hysteresis loops (representing the energy dissipation) are shown in Table 1. The mean, standard deviation (STD), and coefficient of variation (COV) values presented in Table 1 provide a useful summary of the central tendency, variability, and relative variability of the estimated parameters. The model-to-experimental ratio is a measure of the accuracy of the fitted model. A ratio of 1 indicates perfect agreement between the model and the experimental data, while a ratio greater than or less than 1 indicates over-prediction or under-prediction of the model, respectively. The k_L

values and the mean values for k_L estimated using both fitting methods are close to each other (0.98 for all-cycle fitting and 0.99 for one-cycle fitting), indicating that both methods are nearly equally effective in estimating k_L. However, the one-cycle fitting method consistently provides a slightly better estimate of the k_L values compared to the experimental data than the all-cycle fitting method at the same displacement amplitude with the exception of 2.50 t_r.

Generally, the all-cycle fitting method tends to overestimate the energy dissipation capacity of the isolator, resulting in higher area and ζ_L ratios (with ratio ranging between 1.09 to 1.74). The only exception to this trend is observed for the largest displacement amplitude of 2.50 t_r, where the all-cycle fitting method underestimated the energy dissipation capacity of the isolator by 13% (with the ratio of 0.87). In contrast, the one-cycle fitting method provides a more accurate estimation of the isolator's energy dissipation capacity, with ratios closer to 1 and lower error ranges (with ratio ranging from 0.97 to 1.12).

The STD and COV values for k_L, ζ_L, and area are higher for all-cycle fitting compared to one-cycle fitting, indicating that the one-cycle fitting method provides more consistent estimates of these parameters. The higher variability in the all-cycle fitting method is due to the fact that this method uses data from multiple cycles, which results in increased variability in the estimated parameters. It is interesting to note that the estimation error of the area and ζ_L generally decreases with increasing displacement amplitudes (u/t_r) from 0.50 t_r to 2.00 t_r.

The fitted AM model to experimental data using the two methods is shown in Figure 3. Figure 3a shows the model fitted using the all-cycle fitting method, while Figure 3b shows the model fitted using the one-cycle fitting method for 1.50 t_r, 2.00 t_r, and 2.50 t_r cycle. The one-cycle fitted curves for 1.50 t_r and 2.00 t_r exhibit a high degree of visual agreement. However, although the model estimation of the area at the 2.50 t_r cycle to experimental data ratio (1.08) suggests an acceptable level of accuracy, Figure 3b reveals that the model inadequately captures the nuanced softening and stiffening behavior at intermediate displacements. This could potentially sacrifice the model fitting at intermediate displacements for the sake of enhancing experimental fitting at larger displacements.

Table 1. model-to-experimental ratio for all-cycle and one-cycle fitting results.

Cycle (u/t_r)	**all-cycle fitting**			**one-cycle fitting**		
	k_L	ζ_L	**area**	k_L	ζ_L	**area**
0.25	1.08	1.45	1.57	0.98	0.99	0.97
0.50	0.98	1.74	1.71	0.99	1.01	0.99
0.75	0.97	1.72	1.67	0.99	1.00	0.99
1.00	0.98	1.62	1.59	0.99	1.00	0.99
1.50	0.99	1.30	1.29	0.99	1.02	1.01
2.00	0.85	1.28	1.09	0.96	1.12	1.08
2.50	1.00	0.87	0.87	1.02	1.05	1.08
mean	**0.98**	**1.43**	**1.40**	**0.99**	**1.03**	**1.02**
STD	**0.07**	**0.31**	**0.32**	**0.02**	**0.05**	**0.05**
COV (%)	**6.92**	**21.6**	**23.1**	**1.79**	**4.42**	**4.47**

Time-history analysis

To investigate the effect of the two fitting methods on the representation of the hysteretic response of UFREIs, a time history analysis was conducted in OpenSees and compared against the experimental results. The time history analysis results are shown in Table 2 and Figure 4. Table 2 presents the positive and negative peak displacement values for the different levels of PGA. The table presents the experimental values for peak displacement, as well as the values obtained through each fitting method, and the corresponding model-to-experimental ratio. The all-cycle fitting method provides a more precise estimation of the peak displacement values for higher levels of PGA (i.e., 0.3g, 0.4g, and 0.5g), as evidenced by the model-to-experimental ratios, which are closer to unity in the all-cycle fitting method than in the one-cycle fitting method. For example, at a PGA of 0.4g, the ratios for positive and negative peaks are 1.01 and 1.11, respectively, when all-cycle fitting is used, while the ratios for the one-cycle fitting method are 1.18 and 1.16, respectively. On the other hand, the one-cycle fitting method yields more accurate peak values for lower levels of PGA (i.e., 0.1g and 0.2g) than the all-cycle fitting method, with a ratio range of 0.90-1.00 for the former and 0.84-0.94 for the latter. Both methods tend to slightly overestimate the peak displacement values for higher levels of PGA (i.e., 0.3g, 0.4g, and 0.5g), while they tend to underestimate the peaks for lower levels of PGA (i.e., 0.1g and 0.2g), except for the positive peak at 0.3g in the all-cycle fitting, which is underestimated, and 0.2g in the one-cycle fitting, which is overestimated. However, the differences in the model-to-experimental ratios between the two methods are relatively small, ranging from 0.84 to 1.11 for the all-cycle fitting method and from 0.90 to 1.20 for the one-cycle method. However, it is noteworthy that in the case of lower levels of PGA values, the all-cycle fitting approach yields non-conservative results because the peaks at lower amplitudes are underestimated (ratios are lower than 1).

The hysteresis loops of the model, based on the parameters obtained through the all-cycle fitting method, are visibly wider than those obtained through the one-cycle fitting method, particularly at lower levels of PGA values, as illustrated in Figure 4. This implies that the energy dissipation capacity of the isolator is overestimated in the all-cycle fitting method, especially at lower levels of PGA. It is postulated that, in cases where the expected displacement demand is low, the models can be fitted to all lower amplitude cycles only, to improve the overall fit in all cases. Conversely, in cases of high displacement demand, the all-cycle fitting method provides acceptable outcomes.

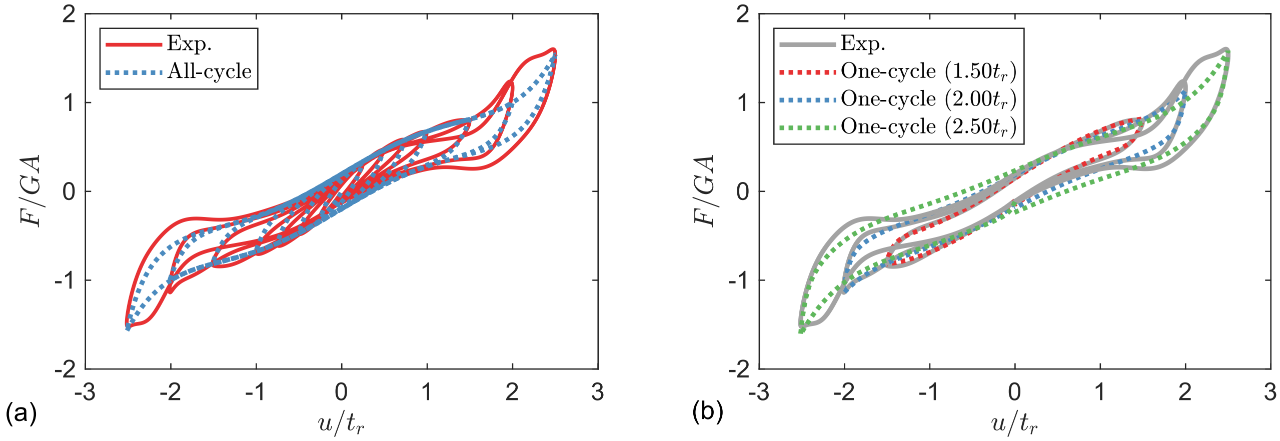

Figure 3. Fitting methods: a) all-cycle fitting and b) one-cycle fitting (fitted to 1.50 t_r, 2.00 t_r, and *2.50 t_r).*

Table 2. Positive and negative peak displacements and model-to-experimental ratio for all-cycle and one-cycle fitting.

PGA	**Exp.**	**All-cycle fitting**		**One-cycle fitting**	
	Peak disp. (t_r)	Peak disp. (t_r)	Ratio	Peak disp. (t_r)	Ratio
0.5g	2.01	2.30	1.14	2.32	1.15
	-2.05	-2.21	1.08	-2.19	1.07
0.4g	1.43	1.45	1.01	1.69	1.18
	-1.28	-1.42	1.11	-1.48	1.16
0.3g	0.98	0.92	0.94	1.18	1.20
	-0.85	-0.85	1.00	-0.89	1.05
0.2g	0.59	0.51	0.86	0.64	1.08
	-0.67	-0.57	0.85	-0.61	0.91
0.1g	0.31	0.26	0.84	0.28	0.90
	-0.34	-0.32	0.94	-0.34	1.00

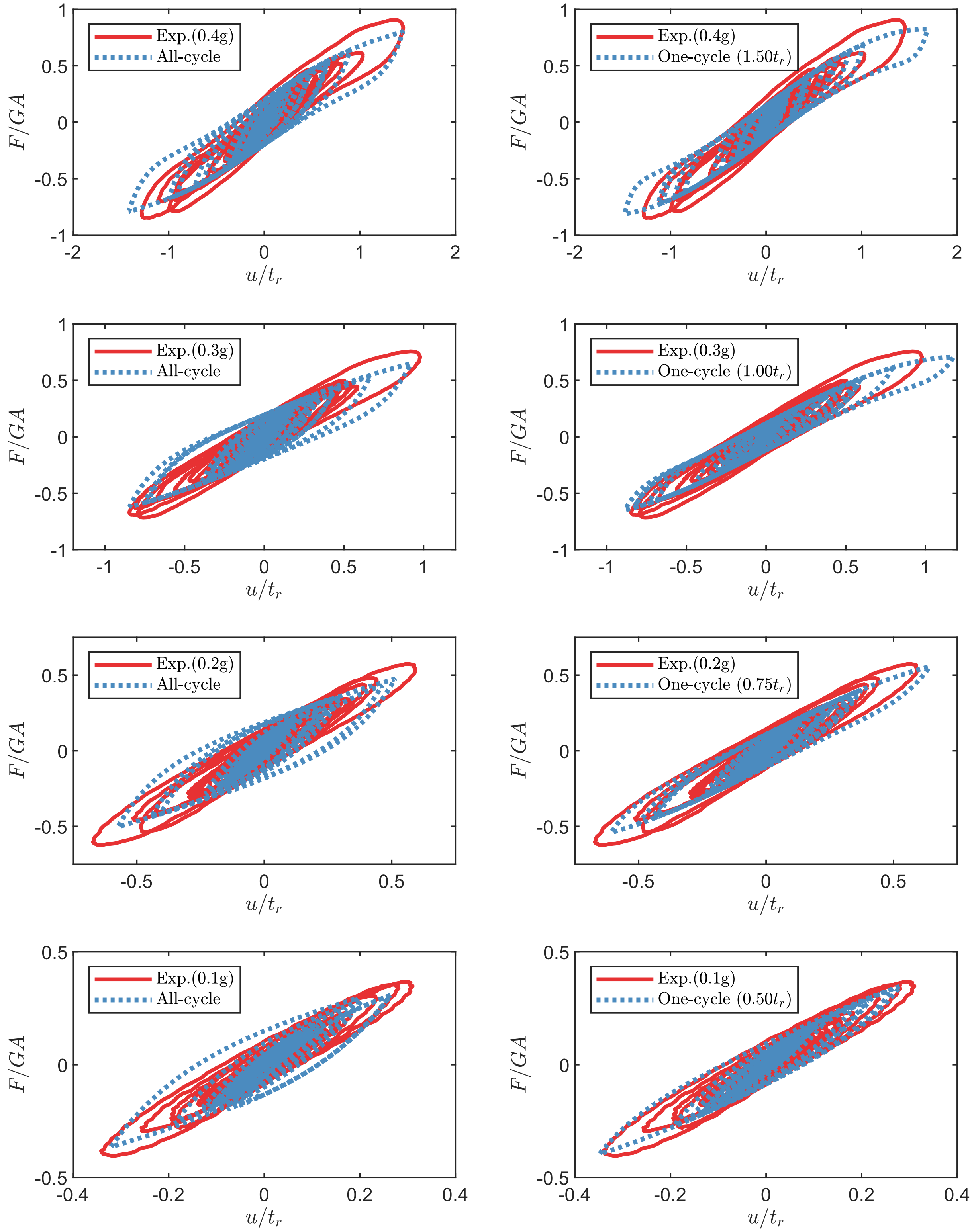

Figure 4. Comparison of the normalized experimental and model hysteretic loops during the El Centro record at 0.1g to 0.4g PGA values; left: all-cycle fitting and right: one-cycle fitting.

CONCLUSIONS

A methodology has been presented to fit a numerical model for UFREI to experimental hysteresis loops obtained from a lateral cyclic loading test. Two methods for fitting the numerical model parameters have been considered: all-cycle fitting and one-cycle fitting (i.e., fitting to the expected displacement demand in earthquake). A time history analysis was conducted using OpenSees software with the parameters derived from the optimization process. The results obtained from the time history analysis have been compared with the shake table test results to investigate the accuracy of each approach. Drawing on the analysis, the following conclusions can be inferred:

- Based on cyclic loading results, the estimated effective lateral stiffness values using both fitting methods are similar, indicating that both methods are equally efficient in k_L estimation. However, the all-cycle fitting method generally overestimates the energy dissipation capacity of the isolator, resulting in higher ratios and wider error ranges. On the other hand, the one-cycle fitting method provides a more accurate estimation with lower error ranges.
- Based on time-history analysis results, for higher PGA levels (0.3g, 0.4g, and 0.5g), the all-cycle fitting method offers a more accurate estimation of peak displacement values compared to the one-cycle fitting method. However, the one-cycle fitting method produces more precise peak values for lower PGA levels (0.1g and 0.2g) than the all-cycle fitting method.
- Lower amplitude cycles can be used to fit models in situations with low expected displacement demand for better results overall, while the all-cycle fitting method is suitable for cases with high displacement demand.
- The all-cycle fitting method produces visibly wider hysteresis loops than the one-cycle method, overestimating the energy dissipation capacity of the isolator, particularly at lower PGA levels.

Note that the results presented in this study are based on a single experimental dataset, one seismic record, and were tested on a single numerical model. Although the employed methodology has exhibited potential in enhancing the precision or reducing the computational effort of numerical models for UFREIs when subjected to seismic loading, further investigations using various experimental tests and different numerical models are imperative to verify and regulate the effectiveness of this approach.

ACKNOWLEDGMENTS

The authors acknowledge the support of the Natural Sciences and Engineering Research Council of Canada (NSERC) [funding reference number RGPIN-2019-03924 and RGPIN-2019-04332]. The undergraduate student was supported by the Undergraduate Research Experience (URE) program at the University of Windsor.

REFERENCES

[1] P. Clemente, "Seismic isolation: past, present and the importance of SHM for the future," *J Civ Struct Health Monit*, vol. 7, no. 2, pp. 217–231, Apr. 2017, doi: 10.1007/s13349-017-0219-6.

[2] N. C. Van Engelen, "Fiber-reinforced elastomeric isolators: A review," *Soil Dynamics and Earthquake Engineering*, vol. 125, 2019, doi: 10.1016/j.soildyn.2019.03.035.

[3] T. C. Becker and S. A. Mahin, "Experimental and analytical study of the bi-directional behavior of the triple friction pendulum isolator," *Earthq Eng Struct Dyn*, vol. 41, no. 3, pp. 355–373, 2012, doi: https://doi.org/10.1002/eqe.1133.

[4] J. Kelly, "Analysis of Fiber-Reinforced Elastomeric Isolators," *Journal of Seismology and Earthquake Engineering*, vol. 2, no. 1, pp. 19–34, 1999.

[5] N. C. van Engelen, D. Konstantinidis, and M. J. Tait, "Structural and nonstructural performance of a seismically isolated building using stable unbonded fiber-reinforced elastomeric isolators," *Earthq Eng Struct Dyn*, vol. 45, no. 3, pp. 421–439, Mar. 2016, doi: 10.1002/EQE.2665.

[6] H. Sheikh, N. C. Van Engelen, and R. Ruparathna, "A review of base isolation systems with adaptive characteristics," *Structures*, vol. 38, pp. 1542–1555, Apr. 2022, doi: 10.1016/J.ISTRUC.2022.02.067.

[7] N. C. van Engelen, M. J. Tait, and D. Konstantinidis, "Model of the Shear Behavior of Unbonded Fiber-Reinforced Elastomeric Isolators," *Journal of Structural Engineering*, vol. 141, no. 7, p. 04014169, Jul. 2015, doi: 10.1061/(ASCE)ST.1943-541X.0001120.

[8] N. Vaiana, S. Sessa, F. Marmo, and L. Rosati, "An accurate and computationally efficient uniaxial phenomenological model for steel and fiber reinforced elastomeric bearings," *Compos Struct*, vol. 211, no. 1, pp. 196–212, 2019, doi: https://doi.org/10.1016/j.compstruct.2018.12.017.

[9] A. Manzoori and H. Toopchi-Nezhad, “Application of an extended Bouc-Wen model in seismic response prediction of unbonded fiber-reinforced isolators,” *Journal of Earthquake Engineering*, vol. 21, no. 1, pp. 87–104, Jan. 2017, doi: 10.1080/13632469.2016.1138166.

[10] R. Bouc, “Forced vibrations of mechanical systems with hysteresis,” in *Fourth Conference on Nonlinear Oscillations*, Prague: Prague, 1967.

[11] Y.-K. Wen, “Method for random vibration of hysteretic systems,” *Journal of the engineering mechanics division*, vol. 102, no. 2, pp. 249–263, 1976, doi: https://doi.org/10.1061/JMCEA3.0002106.

[12] F. Ikhouane and J. Rodellar, *Systems with hysteresis: analysis, identification and control using the Bouc-Wen model*. John Wiley & Sons, 2007.

[13] B. A. D. Foster, “Base isolation using stable unbonded fibre reinforced elastomeric isolators (SU-FREI),” McMaster University, Hamilton, Ontario, 2012.

[14] A. Charalampakis and C. Dimou, “Identification of Bouc–Wen hysteretic systems using particle swarm optimization,” *Computer & Structures*, vol. 88, no. 21–22, pp. 1197–1205, 2010.

[15] M. Millonas, “Swarms, phase transitions, and collective intelligence,” in *Proceeding of Artificial Life*, 1994.

[16] M. Clerc and J. Kennedy, “The particle swarm-explosion, stability, and convergence in a multidimensional complex space,” *IEEE transactions on Evolutionary Computation*, vol. 6, no. 1, pp. 58–73, 2002.

[17] ASCE/SEI 7-22, *Minimum Design Loads and Associated Criteria for Buildings and Other Structures*. American Society of Civil Engineers, 2022. doi: 10.1061/9780784415788.

[18] F. McKenna, M. H. Scott, and G. L. Fenves, “Nonlinear finite-element analysis software architecture using object composition,” *Journal of Computing in Civil Engineering*, vol. 24, no. 1, pp. 95–107, 2010.